Computational Fluid Dynamics Study of Airflow and Particle Transport in Third to Sixth Generation Human Respiratory Tract

Vivek Kumar Srivastav, Akshoy Ranjan Paul and Anuj Jain
Department of Applied Mechanics
Motilal Nehru National Institute of Technology, Allahabad-211004, INDIA.
vivekapril@gmail.com

ABSTRACT

The computational fluid dynamics (CFD) technique is used to simulate airflow and aerosol-particle deposition in human respiratory tract. The three dimensional respiratory tract is extended from third to six generation bronchus based on Weibel model (1963). The computation is performed for laminar flow condition. Discrete phase modeling (DPM) is used to study the two phase flow. The aerosol-particles of three different diameters 1, 5 and 10 μm are considered to obtain the effect of aerosol-particle size on deposition efficiency. The results of velocity contours, aerosol-particle deposition efficiency and aerosol-particle trapping process are determined at different locations of the respiratory tract. It is obtained that deposition efficiency increases with the increase of aerosol-particle size. It is also found that more are deposited at the bifurcation junctions because of the direct inertial impaction at these locations. Computational results are found useful to correlate the medical and engineering aspects.

1. INTRODUCTION

Human respiratory tract is inverted tree like structure that extended from nasal cavity to the alveoli. The main function of respiratory tract is to supply oxygen and carbon dioxide between atmosphere and lungs. In 1963, Weibel reported dimensions of symmetrical lung model based on regular pipes[1]. He extended the lung model from trachea to 23rd generation bronchus. Most of the previous researches frequently used Weibel model[1] because of easy reconstruction [2,3] of respiratory tract. Laminar oscillatory flow in triple bifurcation human respiratory tract was simulated by Zhang et al.[4]. Three realistic breathing conditions (resting, light activity and moderate exercise) were considered in the study. Maximum particle deposition is found at carinal ridges or flow divider during inspiratory flow, however for expiratory flow it observed happened at tubular wall due to strong secondary flow. Both the experimental and computational results show that particle deposition is higher in cyclic flow in comparison to steady flow condition. The airflow study in bifurcated respiratory tract based on Weibel model was carried by Liu et al.[5]. Airflow simulation in fifth to seventh generation respiratory tract was carried out for different Reynolds numbers. They obtained a relation between pressure drop and Reynolds numbers. Nowak et al.[6] compared the airflow and aerosol deposition in two type of airway model: (i) Weibel model and (ii) Computed Tomography (CT) scan model. Steady state inhalation, exhalation as well as unsteady breathing cycles were considered in the study. They compared the aerosol deposition for steady-state and time dependent inhalation conditions and predicted that real breathing circumstances can be captured from time dependent simulation.

Micron particle deposition in CT scan model under different breathing conditions was discussed by Inthavong et al. [7]. It was found that vortex formation in the downstream of bifurcation was responsible for particle deposition.

Particle range of 1 to 10 μm was used by the Radhakrishnan and Kassinos [8]. The research shows that the particles smaller than 1 μm do not deposit at all, since they move by Brownian motion and settle very slowly. And the particles larger than 10 μm deposit in oral cavity or nasal cavity due to inertia. Thus 1-10 μm is the range of particle sizes that have chances of deposition in trachea and lower branches [9, 10, 11].

Researchers [2, 3, 5, 6] have used Weibel model as well as others [6,7, 14, 15] used simulated CT scan model. One of the major drawbacks of CT scan model is surface losses during model construction after fourth/fifth generation. Therefore, Weibel model is generally used for construction of respiratory tract model beyond fourth/fifth generation.

Research [12, 13] shows that toxic-particles are deposited more at the bifurcation junction in comparison of the other locations in respiratory tract causing chronic obstructive pulmonary diseases (COPD). Drugs are used for the immediate relief from COPD and asthma by inhaling aerosol-particles from the rotahaler/Inhaler. The reach and deposition of aerosol-particles at the affected area in respiratory tract governs the efficacy of this treatment. This study is, therefore, focused on the deposition of aerosol particles during inspiratory flow in three dimensional third to sixth generation respiratory tract using Weibel model.

2. GEOMETRY OF HUMAN RESPIRATORY TRACT

The dimension of third to six generation human respiratory tract was adopted from Weibel model[1] and given in table-1. Weibel has established a relation between length and diameter for each associated bronchus. The length-to-diameter ratio for the individual airways element is defined as: $\delta = L/D$, where L and D are the length and diameter of the individual airway. For fourth to tenth generation, value of δ is 3.25[1].

The model was constructed in Ansys-Workbench. The third to six generation off-planar model is shown in Figure 1.Each bronchus is bifurcated at angle of 60 degree. To obtain the deposition efficiency of aerosol-particle and for the analysis of results, total computational domain has been decomposed into several zones as shown in figure.

3. COMPUTATIONAL GRIDS

The computational grid was generated on Ansys-workbench. As tetrahedral elements provide better fitting near the curved surfaces with minimum possible skewness, triangular e mesh was used for the surface meshing and unstructured tetrahedral elements were used for the volume meshing. Boundary adaptation technique in CFD solver was applied for grid refinement. This refinement was repeated until the solution becomes grid-independent as shown in Table 2. It was found that percentage error of both the velocity magnitudes are minimum for case-5 and less than 0.5%. Therefore case-5 for total 1161259 tetrahedral elements was selected for CFD analysis.

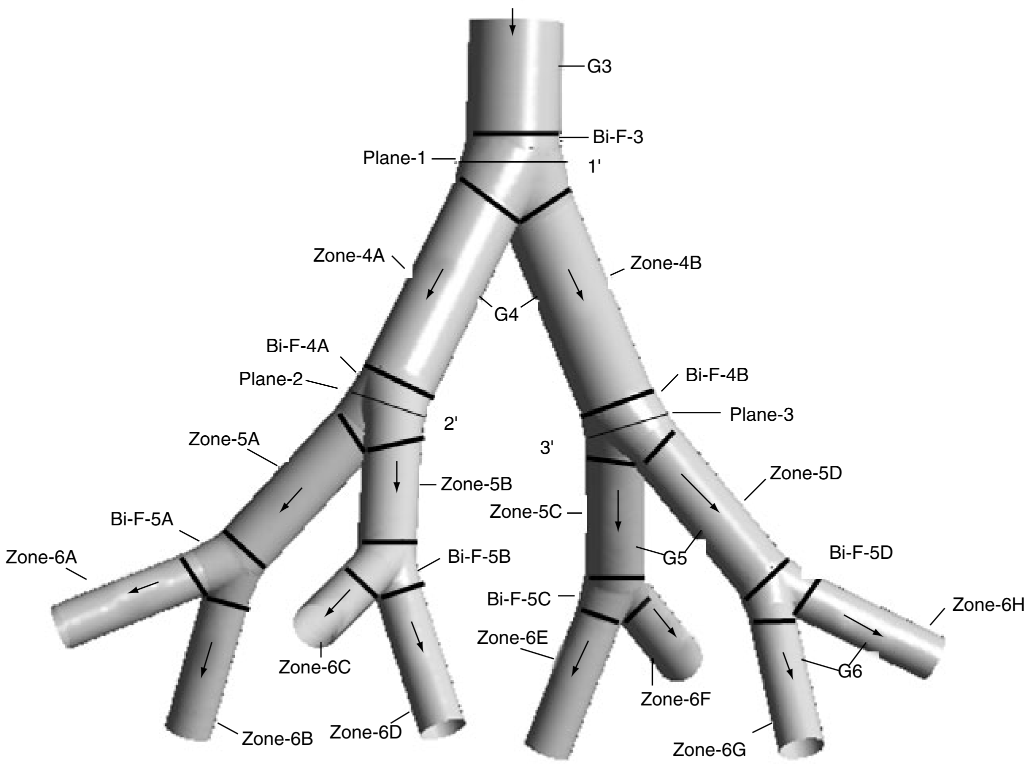

Figure 1. Third to Sixth Generation Human Respiratory Tract (off planar).

Table 1. Respiratory tract dimensions.

Generation	Length (cm)	Diameter (cm)
G3	0.76	0.56
G4	1.27	0.45
G5	1.07	0.35
G6	0.90	0.28

Table 2. Grid Independency Test.

	No. of elements	Max velocity (m/s)	Percentage error	Avg. velocity (m/s)	Percentage error
Case-1	307028	2.76	-	2.038	-
Case-2	527822	2.83	2.4700	2.042	0.2264
Case-3	743625	2.80	1.0400	2.041	0.0497
Case-4	964916	2.77	0.9700	2.045	0.1625
Case-5	**1161259**	**2.78**	**0.3300**	**2.044**	**0.0496**

4. GOVERNING EQUATIONS

The airflow was assumed to be steady and incompressible

Continuity equation:

$$\frac{\partial u_j}{\partial x_j} = 0 \tag{1}$$

Momentum equation:

$$\frac{\partial\left(u_i u_j\right)}{\partial x_j} = -\frac{1}{\rho}\frac{\partial p}{\partial x_i} + \frac{\mu}{\rho}\frac{\partial^2 u_i}{\partial x_i \partial x_j} \tag{2}$$

μ = viscosity coefficient
u_j (i, j = 1, 2, 3) is the velocity component in x, y and z direction.
p = pressure
ρ = density of fluid

Particle Force Balance equation:

Discrete phase model (DPM) has been used for the analysis of aerosol-particle motion in human airway. The equation of motion of particle is obtained by equating the acceleration of particle with forces acting on the particle per unit mass as given below:

$$\frac{\partial u_p}{\partial t} = F_D(u - u_p) + \frac{g_x(\rho_p - \rho)}{\rho_p} \tag{3}$$

First term on right hand side of equation represents drag force and second term gravitational force. Where F_D is define as:

$$F_D = \frac{18\mu}{\rho_p d_p^2}\frac{C_D \mathrm{Re}}{24} \tag{4}$$

u is the fluid phase velocity, u_p is the particle velocity, μ is the molecular viscosity of fluid, ρ is the fluid density, ρ_p is the density of the particle, and d_p is the particle diameter. Re is the relative Reynolds number, which is defined as:

$$Re \equiv \frac{\rho d_p \left| u_p - u \right|}{\mu} \tag{5}$$

The drag coefficient (C_D) formula can be calculated from $C_D = a_1 + \frac{a_2}{Re} + \frac{a_3}{Re^2}$ (6)

Where a_1, a_2 and a_3 are constants that apply to smooth spherical particles over several ranges of Re[16].

5. BOUNDARY CONDITIONS

The mass flow rate and pressure out conditions were applied at the inlet of third generation bronchus and eight outlets of six generation bronchi respectively. The flow rate at the inlet of third generation bronchus is 3.53 L/min corresponding to inlet flow rate 28.3 L/min at trachea adopted from Nowak et al.[6]. The properties of air at normal conditions were considered in this study, i.e., density 1.19 kg/m^3 and viscosity 1.82×10^{-5} kg/m-s. The aerosol-particles , having diameters of 1, 5 and 10 μm and density equivalent to water (1000 kg/m^3) is used in this study. Two different boundary conditions are used in Discrete Phase Model (DPM). Escape option in ANSYS-FLUENT was enabled at inlet and outlets, while trap option enabled for walls.

6. NUMERICAL SIMULATION

Ansys Fluent was used for the simulation of airflow and aerosol-particle deposition in third to six generation human airway model. The pressure term of the transport equation was discretised using second order upwind scheme and momentum term using QUICK scheme. The SIMPLEC algorithm was applied in CFD solver for the pressure-velocity coupling. Convergence criteria equivalent to 10^{-4} was taken in this study. The computational work was run on IBM Workstation with 8GB RAM.

7. COMPUTATIONAL VALIDATION

The present work has been validated against the experimental and computational air velocities reported by Nowak et al. [6] and Zhao & Leiber [17] respectively. The relative velocity profile across diameter at the mid plane of brochus-4(G4) is plotted along with the result of Nowak et al. [6] and Zhao & Leiber [17] in Figure 2.

8. RESULTS AND DISCUSSION

8.1. Velocity contours at bifurcation junction

The iso-velocity contours are plotted at three bifurcation junctions (bifurcation junction-3, 4A and 4B) in Figure-3. The velocity contour at bifurcation junction-3 is plotted at plane-1-1′ as shown in Figure 1. The higher velocities are found close to dividers near the inner wall of next generation bronchi . The symmetric contour patterns for this plane is obtained because the velocity at the inlet of third generation was taken as uniform. . Since the particles are driven by the airflow patterns, more particles are expected to be deposited at curved surface of bifurcation junctions. Maximum particle deposition is likely to occur at dividers (or bifurcation junction) due to direct inertial impaction.

The velocity contours for the bifurcation junction-4 are drawn at plane-2-2′ and 3-3′ in Figure-3. The velocity contour plots for plane-2-2′ and 3-3′ are different as compared to plot for plane 1-1′ because off-plane 3-D construction of respiratory tract. Higher velocity gradient is observed near inner wall (2′ and 3′) as compared to that of near outer wall (2 and 3)

Thus, velocity contours provide an idea of particle deposition in the respiratory tract.

8.2. Effects of particle size on deposition efficiency

The three different aerosol-particles of size 1, 5 and 10 micron are injected at the inlet of third generation bronchus. The deposition efficiency is defined as:

Deposition efficiency = (Number of particle deposited at a particular zone/total number of aerosol-particles injected at the inlet of third generation bronchus) × 100.

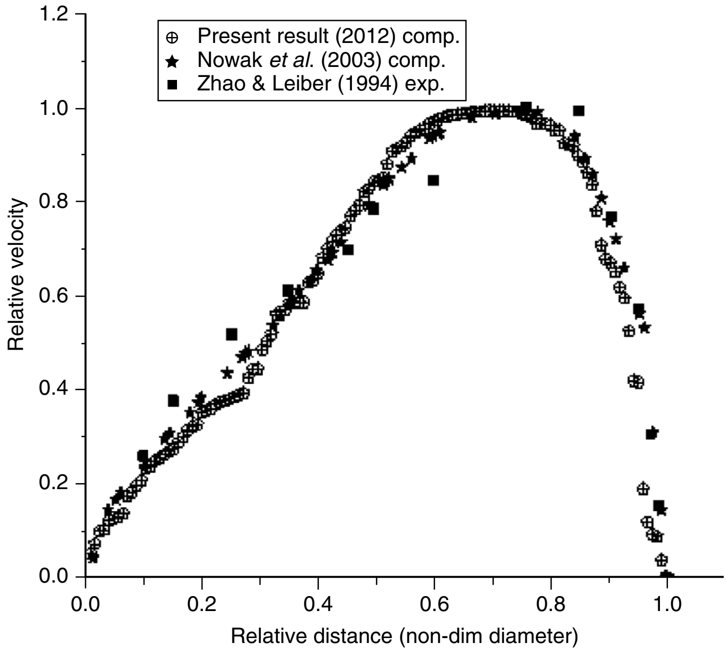

Figure 2. Velocity profile at midpoint of generation–4(G4).

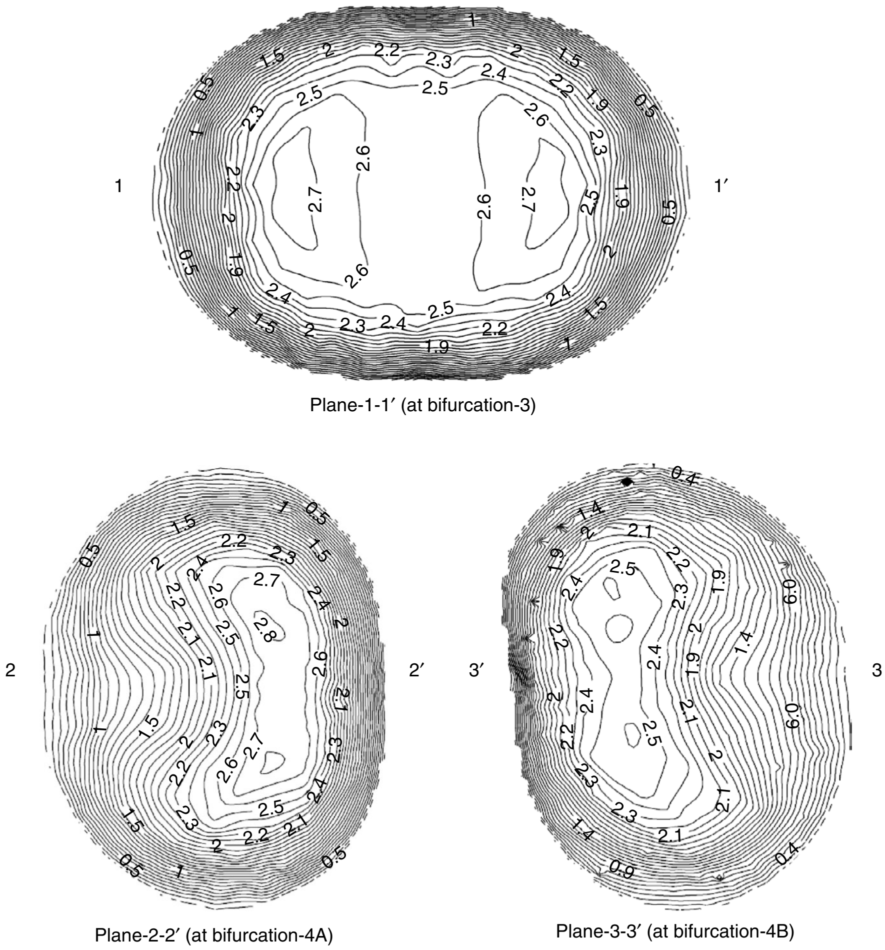

Figure 3. Velocity Contours (m/s) at Bifurcation Junctions

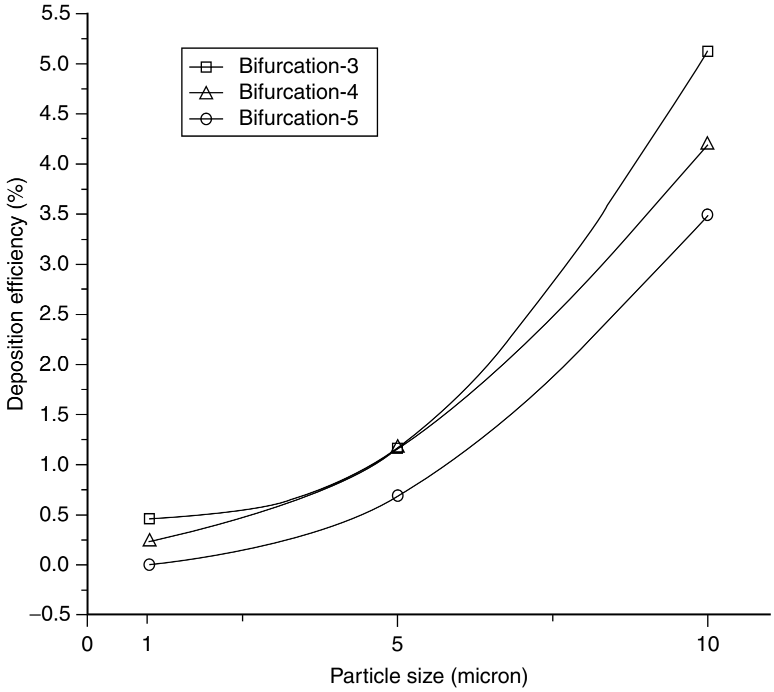

Figure 4: Aerosol-Particle Size vs Deposition Efficiency

The deposition efficiency is calculated for Bifurcation junction-3, Bifurcation junction-4 (sum of 4A and 4B), and Bifurcation junction-5 (sum of 5A, 5B, 5C and 5D) and shown in Figure-4.The deposition efficiency increases with increase in size of aerosol-particle. Maximum deposition efficiency is occurred at bifurcation-3 for 10 micron aerosol-particle size. But this deposition efficiency decreases as aerosol-particles moves towards the lower bifurcations.

8.3. Deposition efficiency at bronchus and bifurcation junction

The maximum deposition is obtained for 10-micron size aerosol-particles, therefore further results are analyzed for 10-micron size aerosol-particles . Aerosol-Particle deposition at different zones of bronchi and bifurcations is shown in Table-3. The total deposition from third bifurcation (Bi-F-3) to the outlet of sixth generation bronchi is found 25.36%.

Since the bronchi of particular generation are symmetrical about its bifurcation, having length and diameter same therefore, aerosol-particle deposition is same for each symmetrical bronchus. Fourth generation bronchus is divided into two symmetrical zones (zone-4A & zone-4B, Table-3). 1.86% of aerosol-particles are deposited at each bronchus of generation four (Table-3). Fifth generation bronchus is divided into four symmetrical zones (zone-5A, zone-5B, zone-5C & zone-5D). It has been found that the deposition efficiency decreases as aerosol-particles moves towards the lower bronchus.

Table 3. Aerosol-particles Trapped at Different Zones

Zones	Percentage of deposited particles (%)
Bi-F-3	5.12
zone-4 (A+B)	3.72
Bi-F-4	3.49
zone-5(A+B+C+D)	5.11
Bi-F-5 (A+B+C+D)	4.19
Sum (Zone-6A to 6H)	3.73
Total deposition	**25.36**

Because of the direct impaction of the aerosol-particle at the bifurcation junction, more particles are deposited at this location as compared to particles at the wall of bronchi(Table-3). Maximum aerosol-particle deposition efficiency (5.12%) is obtained at the bifurcation junction-3(Bi-F-3).

8.4 Aerosol-particle Trapping Process

The aerosol-particle trapping/deposition process is given in figure 5. The article deposition process is depicted in four time steps. Step-1 shows the particles velocity when they cross bifurcation junction-1 and reach bifurcation junction-2. Dark blue color particles represent particles at zero velocity and indicate trapped particles. Step-1 reveals that the particles are deposited at the bifurcation junction-3.

Step-2 shows advancement of the particles as they reached at bifurcation-5. Step-2 depicts that the particles are deposited on outer wall of bronchi of generation 4 near bifurcation junction 3. Step-3 indicates that more particles are deposited at outer wall as compared to inner wall of the bronchi of generation 4. Similar results are observed for the following generations and bifurcations in subsequent steps. The figure also shows that, as the particles moves in the subsequent generation bronchi, the velocity of aerosol-particle reduces.

It is clear from aerosol-particle distribution that bifurcation junction has maximum probability of trapping comparison of other locations of the tract. The deposition of the aerosol-particle decreases in the subsequent bronchi of respiratory tract as aerosol-particles moves towards lower bronchi.

9. CONCLUSIONS

The airflow and aerosol-particle deposition in three dimensional human respiratory tract is simulated for laminar flow condition. The distribution of aerosol-particle deposition at different locations of the airway model is analyzed. The conclusions are given below:

1. It is found that aerosol-particle deposition efficiency typically decreases from bifurcation-to-bifurcation and bronchus to subsequent bronchus.

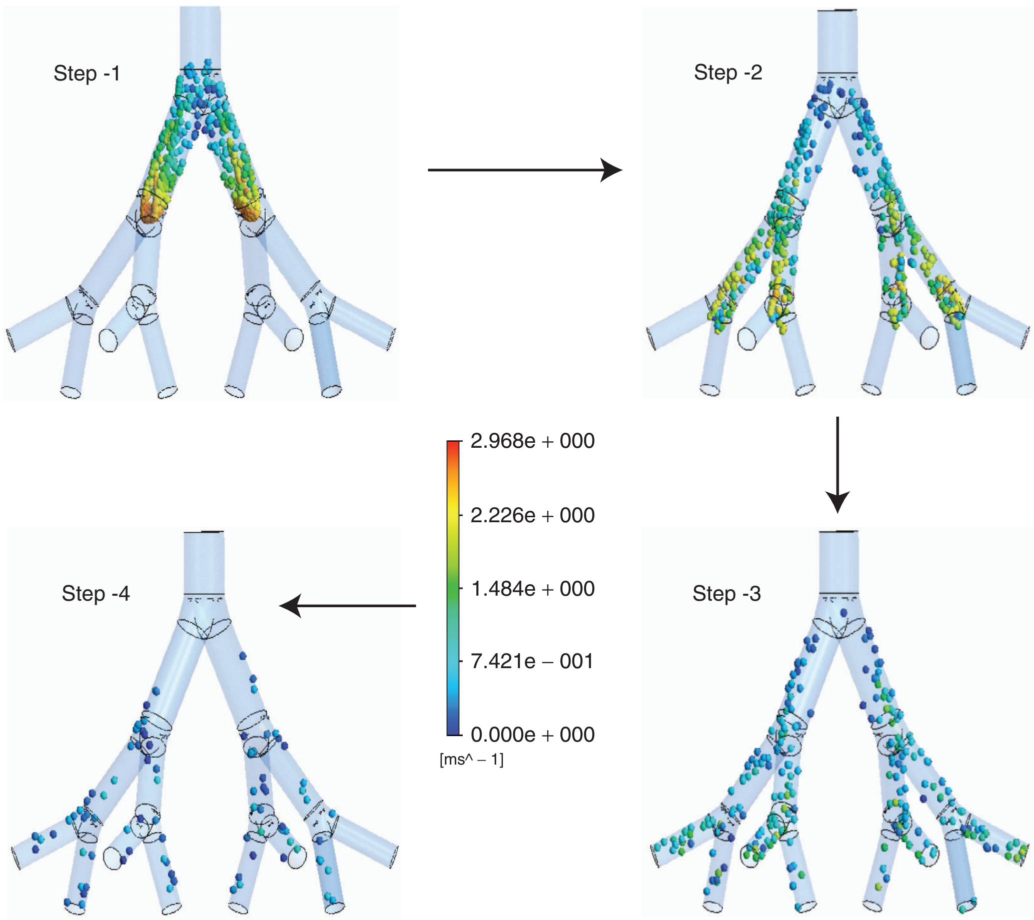

Figure 5: Aerosol-Particle Deposition Processes of Respiratory Tract

2. More aerosol-particles are deposited at the bifurcation junction as compared to that on the walls of subsequent bronchi. .
3. The dose and design of the rotahaler/inhaler can be decided on the basis of these studies.Results will be useful to improve the inhalation treatment through inhaler.

ACKNOWLEDGEMENT

The computation facility used in this study was funded by Department of Science & Technology Government of India through the DST-FIST grant. The authors would like to acknowledge the help rendered by Prof. Ewald R. Weibel, University of Berne, Switzerland by providing some of his key research papers on this topic.

REFERENCES

[1] E. R. Weibel. *Morphometry of human lungs*. Springer Verlag and Academic Press, Berlin, New York, 1963.

[2] C. Kleinstreuer and Z. Zhang, *Airflow and Particle Transport in the Human Respiratory System*. Annual Review, Fluid Mech, 2010, **42**, 301–334.

[3] D. Yijuan, F. Minrui, X. Sun, and T.C.Yang, *Modeling of the Human Bronchial Tree and Simulation of Internal Airflow: A Review*. K. Li et al. (Eds.), 2010, 456–465.

[4] Z. Zhang, C. Kleinstreuer, C.S. Kim, *Gas–solid two-phase flow in a triple bifurcation lung airway model*. International Journal of Multiphase Flow, 2002, **28**, 1021–1046.

[5] Y. Liu, R.M.C. So, C.H. Zhang, *Modeling the bifurcating flow in a human lung airway*. Journal of Biomechanics, 2002, **35**, 465–473.

[6] N. Nowak, P. P. Kakade and A. V. Annapragada, *Computational Fluid Dynamics Simulation of Airflow and Aerosol Deposition in Human Lungs*. Annals of Biomedical Engineering, 2003, **31**, 374–390.

[7] Kiao Inthavong, Choi Lok-Tin, Tu Jiyuan, Ding Songlin, Thien Francis, *Micron particle deposition in a tracheobronchial airway model under different breathing conditions*. Medical Engineering & Physics, 2010, **10**, 1198–1212.

[8] H. Radhakrishnan and S. Kassinos, *CFD Modeling of Turbulent Flow and Particle Deposition in Human Lungs*. 31st Annual International Conference of the IEEE EMBS, Minneapolis, Minnesota, USA, September 2–6, 2009.

[9] MA Baoshun and R. L. Kenneth, *CFD Simulation of Aerosol Deposition in an Anatomically Based Human Large–Medium Airway Model*. Annals of Biomedical Engineering, 2009, **37**, 271–285.

[10] M. J. Telko and A. J. Hickey, *Dry Powder Inhaler Formulation*. Respiratory Care, 2005, **50**, 1209-1227.

[11] V. K. Srivastav, A. Jain, A. R. Paul, S Joshi. *CFD Modelling of Airflow in Human Respiratory System. International Conference on Mechanical Engineering (ICME-2011)*, Dec.18-20, 2011, Dhaka, Bangladesh. ICME-11-FL-009.

[12] Z. Zhang, C., Kleinstreuer and C. S. Kim, Airflow and Nanoparticle Deposition in a 16-Generation Tracheo bronchial Airway Model. *Annals of Biomedical Engineering*. 2008, 36, 2095–2110.

[13] X. G. Zhao, X. X. Xu, SH. L.Tan, Y. J. Liu, ZH. H. *Gao. Characteristic of Gas-Solid Two-Phase Flow in the Human Upper Respiratory Tract Model*. IEEE. 2009.

[14] V. K. Srivastav, A. R. Paul, A. Jain. Effects of Cartilaginous Rings on Airflow and Particle Transport through Simplified and Realistic Human Upper Respiratory Tracts. To be published in *Acta Mechanica Sinica*. *Manu*. No.: ams2013-036 (Accepted).

[15] V. K. Srivastav, A. Kumar, S. K. Shukla, A. R. Paul, A. D. Bhatt, A. Jain. Airflow and Aerosol-Drug Delivery in a CT Scan based Human Respiratory Tract with Tumor using CFD. *Journal of Applied Fluid Mechanic*. To be published in Vol 7(2), 2014.

[16] S. A. Morsi and A. J. Alexander. An investigation of particle trajectories in two-phase flow systems. *J. Fluid Mech*. 1972. 55, 193–208.

[17] Y. Zhao, and B. B. Lieber. Steady inspiratory flow in a model symmetrical bifurcation. *J. Biomech. Eng*., 1994, 116, 488–496.